Full Paper
doi.org/10.1002/chem.202000132

Protein Function

Flexibility of the CueR Metal Site Probed by Instantaneous Change of Element and Oxidation State from Ag^{I} to Cd^{II}

Ria K. Balogh,[b] Béla Gyurcsik,[b] Mikael Jensen,[c] Peter W. Thulstrup,[a] Ulli Köster,[d] Niels Johan Christensen,[e] Frederik J. Mørch,[a] Marianne L. Jensen,[f] Attila Jancsó,*[b] and Lars Hemmingsen*[a]

Abstract: Selectivity for monovalent metal ions is an important facet of the function of the metalloregulatory protein CueR. ^{111}Ag perturbed angular correlation of γ-rays (PAC) spectroscopy probes the metal site structure and the relaxation accompanying the instantaneous change from Ag^{I} to Cd^{II} upon ^{111}Ag radioactive decay. That is, a change from Ag^{I}, which activates transcription, to Cd^{II}, which does not. In the frozen state (−196 °C) two nuclear quadrupole interactions (NQIs) are observed; one (NQI_1) agrees well with two coordinating thiolates and an additional longer contact to the S77 backbone carbonyl, and the other (NQI_2) reflects that Cd^{II} has attracted additional ligand(s). At 1 °C only NQI_2 is observed, demonstrating that relaxation to this structure occurs within ≈10 ns of the decay of ^{111}Ag. Thus, transformation from Ag^{I} to Cd^{II} rapidly disrupts the functional linear bis(thiolato)Ag^{I} metal site structure. This inherent metal site flexibility may be central to CueR function, leading to remodelling into a non-functional structure upon binding of non-cognate metal ions. In a broader perspective, ^{111}Ag PAC spectroscopy may be applied to probe the flexibility of protein metal sites.

Introduction

Maintaining the intracellular concentration of metal ions at an optimal level is important for all organisms. For example, the copper homeostasis of *Escherichia coli* is managed partially by the *cue* system including CopA, CueO and CueR proteins.[1,2] CopA is a P-type ATPase, transporting Cu^{I} ions into the periplasmic space. CueO is a periplasmic multicopper oxidase that converts Cu^{I} to less harmful Cu^{II}.[3] CueR functions as a transcriptional metalloregulatory protein.[4] Under normal conditions, apo-CueR is bound to the promoter region of the *cue* operon. Upon cognate metal ion binding, it activates the transcription of the downstream *copA* and the *cueO* genes.[1,2,4]

CueR belongs to the MerR metalloregulatory family sharing the common fold of the dimeric structure. The main units are: an N-terminal winged helix DNA binding domain, followed by a dimerization helix and a C-terminal metal binding domain (Figure 1 A).[5,6] The C-terminal region of MerR family proteins is more diverse in terms of sequence and structure than the other segments and this region is responsible for the recognition of various types of effectors, including metal ions.[7–9] Crystal structures of the metal ion bound form of the MerR,[10,11] ZntR,[5] CueR[5,6] and CadR[12] proteins suggest that the metal ion binding region of MerR proteins has evolved to provide an appropriate number and geometry of ligands for the regulated metal ions.[8] In addition, other residues surrounding the metal site may influence the metal ion recognition through charge neutralization, hydrophobic or steric restrictions.[8,13]

CueR activates the transcription only in the presence of the monovalent group 11 transition metal ions Cu^{I}, Ag^{I} and Au^{I}.[4,5,14] These cognate metal ions bind to two cysteine thiolates (C112, C120) of the metal binding loop in a linear coordination geometry (Figure 1 B).[5,6] The structure of the Ag^{I}-bound activator form of CueR co-crystallized with DNA[6] shows that DNA binding does not alter the coordination characteristics of the metal ion to the protein.

[a] Prof. P. W. Thulstrup, F. J. Mørch, Prof. L. Hemmingsen
Department of Chemistry, University of Copenhagen
Universitetsparken 5, 2100 Copenhagen (Denmark)
E-mail: lhe@chem.ku.dk

[b] R. K. Balogh, Prof. B. Gyurcsik, Prof. A. Jancsó
Department of Inorganic and Analytical Chemistry
University of Szeged, Dóm tér 7, 6720 Szeged (Hungary)
E-mail: jancso@chem.u-szeged.hu

[c] Prof. M. Jensen
Hevesy Laboratory, DTU-Health, Technical University of Denmark
Frederiksborgvej 399, 4000 Roskilde (Denmark)

[d] Dr. U. Köster
Institut Laue-Langevin, 71 avenue des Martyrs, 38042 Grenoble (France)

[e] Prof. N. J. Christensen
Department of Chemistry, Faculty of Science, University of Copenhagen
Thorvaldsensvej 40, 1871 Frederiksberg C (Denmark)

[f] M. L. Jensen
Niels Bohr Institute, University of Copenhagen
Universitetsparken 5, 2100 Copenhagen (Denmark)

Supporting information and the ORCID identification number(s) for the author(s) of this article can be found under: https://doi.org/10.1002/chem.202000132.

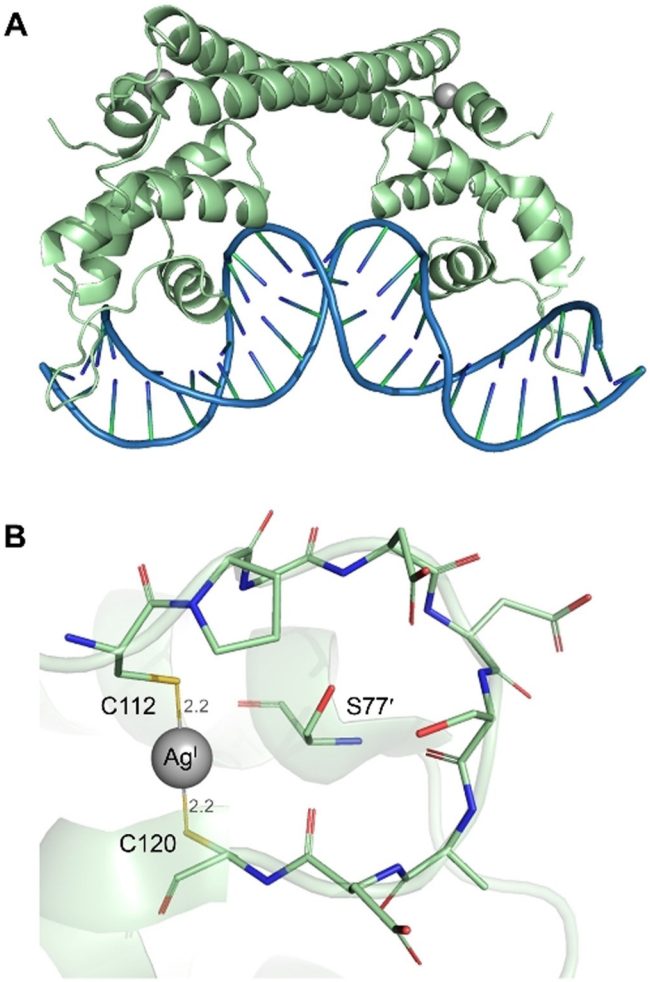

Figure 1. A) Overall structure of the activator form of CueR (PDB ID: 4WLW).[6] Ag^{I} ions are shown as grey spheres. B) Close-up view of the metal binding loop. Residues from C112 to C120 of one monomer, and S77 of the other monomer are indicated explicitly. Ag^{I} is coordinated by C112 and C120 in a linear dithiolate fashion.

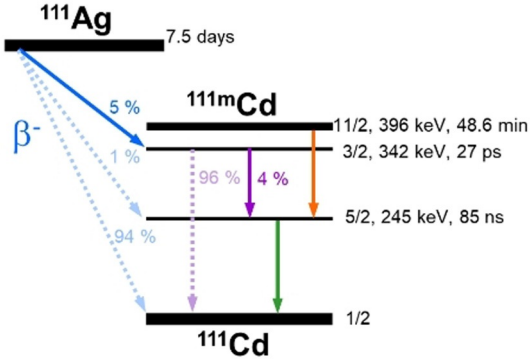

Figure 2. Decay schemes of ^{111}Ag and ^{111m}Cd including information about the nuclear spin, the energy and the half-life of the energy levels. The solid arrows indicate the γ–γ-cascade used in PAC spectroscopy. Notice that the ^{111}Ag and ^{111m}Cd decay pass through the same intermediate state ($I = 5/2$), and it is the NQIs experienced by the Cd nucleus in this state, that are recorded in ^{111}Ag and ^{111m}Cd PAC spectroscopy.

Analysis of the electrostatic- and hydrogen-bonding interactions in the crystal structure suggested that the net negative charge of the S-Cu-S centre might be partly neutralized by a helix dipole and a fairly distant lysine residue.[5] Furthermore, the S77 residue of the other monomer was found to interact with the C112 and D115 residues of the metal binding loop stabilizing its structure.[5,15]

In this work, the structure and flexibility of the metal ion binding site of the Wild Type *E. coli* CueR was probed by ^{111}Ag and ^{111m}Cd perturbed angular correlation of γ-rays (PAC) spectroscopy.[16,17] The radioactive decay of ^{111}Ag is described in some detail here, as a prerequisite for the interpretation of the PAC spectroscopic data in terms of metal site structure. ^{111}Ag decays by β^- emission to ^{111}Cd, and with a ≈5% probability an excited state of the ^{111}Cd nucleus (342 keV) is populated (Figure 2). This state may decay by successive emission of two γ-rays, thereby providing the γ–γ cascade required for PAC spectroscopy.[16] The intermediate (245 keV) level in this γ–γ cascade has a half-life of 85 ns, and it is the nuclear quadrupole interactions (NQI) experienced by the Cd nucleus in this state that are recorded in the ^{111}Ag PAC experiments. Accordingly, the observed spectra may reflect one of three possible scenarios: 1) structural relaxation from the Ag^{I} coordination geometry to that of Cd^{II} occurs rapidly (faster than ≈10 ns), and the ^{111}Ag PAC experiments reflect the relaxed structure, 2) relaxation occurs on the PAC time scale (10–200 ns), and the recorded NQIs change as a function of time on this ns time scale, or 3) the relaxation is slower than ≈200 ns, and the coordination geometry of Ag^{I} is observed.

An instantaneous change of element and oxidation state from Ag^{I} to Cd^{II} accompanies the decay of ^{111}Ag, see above. Moreover, in the nuclear decay the Cd nucleus receives a recoil energy corresponding to the momenta of the emitted β^- and antineutrino. The continuous spectrum of ^{111}Cd recoil energies in the β^- decay of ^{111}Ag extends up to a maximum of 557 kJ mol^{-1}, but the phase space for such high values is negligibly small. In fact, the recoil energies are typically smaller by a factor of 2 or more. Due to the change of element, change of redox state, and the recoil energy, the system is shifted out of equilibrium, and the subsequent relaxation process reflects the rigidity/flexibility of the metal site. In the current case the change from Ag^{I} to Cd^{II} is particularly interesting, because it is a change from a metal ion which induces activation of transcription (Ag^{I}) to a metal ion which does not (Cd^{II}). Moreover, while both metal ions favour the binding of thiolate donors, the AgS_2 coordination mode is highly unusual for cadmium, and linear coordination geometry is only observed for $CdMe_2$ and the dihalides in the gas phase.[18–20] Thus, a fundamental question is if the CueR metal site is sufficiently rigid that Cd^{II} remains transiently in the linear two-coordinate structure, or if the preference of Cd^{II} for higher coordination numbers dominates and leads to remodelling of the metal site coordination geometry. In a broader perspective, ^{111}Ag PAC spectroscopy provides insight into the local potential energy minima that may be realized at protein metal sites by the change from Ag^{I} to Cd^{II} and its initial recoil kinetic energy. This local metal site adaptability/rigidity is likely to be an important facet—beyond

structure—of metalloprotein function, and it is related to the so-called entatic state proposed to account for the properties of e.g. Type 1 Cu centres in blue copper proteins.[21–23]

Results and Discussion

The bacterial metalloregulator protein CueR discriminates very effectively between mono- and divalent metal ions. It is a central tenet that the selectivity is achieved by the unique two-coordinated site occupied by Cu^{I}, Ag^{I} and Au^{I}, while divalent metal ions usually require higher coordination numbers.

Initially we conducted experiments on Ag^{I}-CueR at −196 °C to prevent or slow down the structural relaxation occurring after the decay of ^{111}Ag to ^{111}Cd. Two NQIs were observed, see Figure 3. The high frequency NQI_1 is analysed unambiguously, given that all three peaks characteristic of a ^{111}Ag PAC signal rise above the noise level, and they satisfy the requirement $\omega_1+\omega_2=\omega_3$.[16] The second NQI_2 is characterized by a lower frequency, and we present the best fit in Table 1. Analysing the first 100 ns of the PAC data gives essentially the same two NQIs as analysis of the data from 100 to 200 ns after the decay. This indicates that no structural changes occur within the time span from ≈10 to 200 ns after the decay, and we therefore rule out structural relaxation on the 10–200 ns time scale. That is, the two observed NQIs reflect structures which are stable on the PAC time scale (up to ≈200 ns) at a temperature of −196 °C.

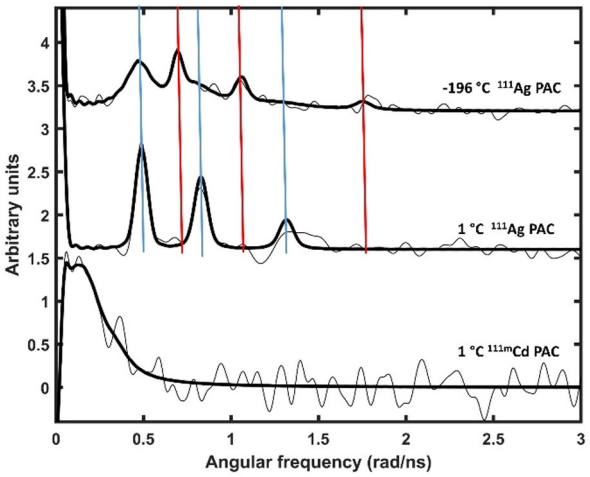

Figure 3. ^{111}Ag- and ^{111m}Cd-PAC spectra of CueR. Top: at −196 °C two different NQIs characterized by a high frequency signal (red), NQI_1, and a low frequency signal (blue), NQI_2, are observed; Middle: at 1 °C only the low frequency signal, NQI_2, is observed; Bottom: the ^{111m}Cd-PAC spectrum of Cd^{II} bound to CueR gives a very low frequency signal. The experimental ^{111}Ag data are multiplied by −1 to allow for comparison to the ^{111m}Cd PAC data. Experimental and fitted data are shown by thin and thick black lines, respectively. $c_{CueR}=11$ μM, $c_{Ag^I}=5.5$ μM, $c_{Cd^{II}}=11$ μM, $c_{DNA}=5.5$ μM, *w/w*%$_{sucrose}=55$%, pH = 7.3 at room temperature.

Table 1. Parameters fitted to the ^{111}Ag PAC and ^{111m}Cd PAC-data for CueR. The rotational correlation time was fixed to infinite at −196 °C because it is assumed that the protein is completely immobilized. See reference [16] for a description of the parameters.

Isotope	*T* [°C]	ω_0 [rad ns^{-1}]	η	δ ×100	$1/\tau_c$ [μs^{-1}]	*A* ×100	χ_r^2
^{111}Ag	−196	0.555(2)	0.510(8)	2.5(6)	0(fix)	−2.3(4)	0.93
		0.41(1)	0.39(4)	16(2)	0(fix)	−7.4(1)	
^{111}Ag	1	0.426(1)	0.384(6)	1.5(6)	6(4)	−6.3(6)	0.90
^{111m}Cd	1	0.11(2)	0.5(5)	9(14)	6(4)	9(2)	0.78

The high frequency signal is relatively straightforward to interpret in terms of metal site structure. Both semi-empirical AOM[24] and DFT calculations indicate that Cd^{II} remains essentially in the Ag^{I} coordination geometry, see Figure 4, possibly establishing a long contact (2.59 Å) with the S77 carbonyl oxygen. An overlay with the Ag^{I}-CueR crystal structure is presented in Figure S5 (Supporting Information), illustrating that the protein atoms move very little, whereas Cd^{II} shifts by ≈0.7 Å towards the Ser77 carbonyl oxygen. The significant deviation of the asymmetry parameter from zero ($\eta=0.51$) indicates that the structure is distorted, that is, the linear coordination observed in the crystal structures is not maintained, but the very high frequency ($\omega_0=0.555$ rad ns^{-1}) agrees well with coordination by two thiolates and no coordinating ligands in the equatorial plane. Typical Cd–O bond lengths for a carbonyl oxygen found in the Cambridge Structural Database are in the range of 2.24–2.41 Å,[12] and are expected to be even shorter for the 2–3 coordinate Cd^{II} observed in this work. Thus, the long contact given by the constrained DFT geometry optimization, Figure 4, is clearly beyond normal bond length. That is, this signal reflects distorted linear bis(thiolato)Cd^{II} with an additional interaction with the carbonyl oxygen of S77.

The other signal, NQI_2, is more difficult to interpret unambiguously because several possible structures map into the observed frequency range. However, the lower frequency relative to NQI_1 strongly indicates a coordination number higher than 2, either as a result of coordination by a nearby amino acid residue or an extraneous ligand such as a solvent water molecule. Finally, there is a minor fraction (<10%) of the signal that is fitted as an exponential decay of the perturbation function.

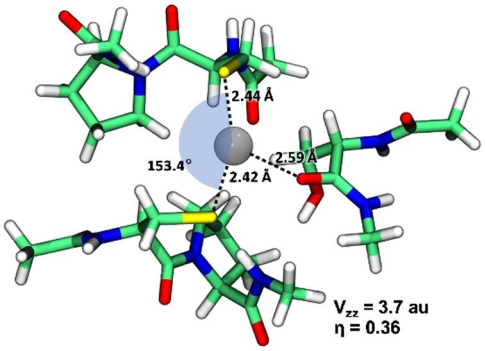

Figure 4. Geometry-optimized metal site structure with Cd^{II} at the CueR metal site (BP86-D3BJ/def2-TZVP) and calculated electric field gradient (EFG) parameters (DKH2 Hamiltonian, BHandHLYP with def2-QZVPP on Cd^{II} and def2-TZVP on remaining atoms), see the text for details. The S-Cd^{II}-S angle is indicated in transparent blue. The EFG parameters derived from the experimental data presented in Table 1 for NQI_1 are: $V_{zz}=3.9$ au and $\eta=0.51$ in fair agreement with the calculated EFG (using $Q=0.64$ barn for the intermediate nuclear level of ^{111}Cd)[25]. Coordinates for the optimized geometry are included in the Supporting Information.

This may reflect Cd^{II} ions ejected from the metal site due to the recoil energy in the β-decay, see above, and this small fraction of the signal is therefore affected either by dynamics or unspecific binding. There are two possible explanations of the observation of the two well defined NQIs (NQI_1 and NQI_2), indicated hereafter as Scenario A and B.

Scenario A: There are two co-existing coordination geometries for Ag^{I} bound to the CueR metal site. One of the signals (NQI_1) would then reflect that Cd^{II} remains in the $CdS_2(O)$ structure (indicating that there is a long contact to the carbonyl oxygen of S77). The other could involve coordination by a water molecule or another extraneous ligand, giving rise to NQI_2. A coordination number of 3 at the CueR metal site is in conflict with the EXAFS and XANES data measured for the Cu^{I}-CueR complex,[26] although it is conceivable that the XANES data would exhibit the characteristic 1s to 4p transition at 8983 eV even upon bending of the S-Cu^{I}-S unit.[27] Thus, a structure similar to that presented in Figure 4, with a remote equatorial oxygen ligand might exist. The similarity of the Cu^{I}-CueR XANES spectra to those of the linear model complex presented by Chen et al.[26] is however striking, making the alternative interpretation of a bent CuS_2 structure unlikely. An alternative structural interpretation may be inspired by our previous suggestion for the CueR metal site with one of the cysteines coordinating in the protonated form.[15] Within this model, it is conceivable that the low frequency signal could originate from a species where Ag^{I} is coordinated by one thiolate and one thiol. If so, a pH dependent change is expected for the relative intensities of the low and high frequency signals, reflecting the pK_a of the coordinated thiol. In order to explore if this type of protonation equilibrium exists, we carried out a pH series (pH 5.7–8.0) of ^{111}Ag PAC experiments. The data do not exhibit any clear pH dependence, see Figure S1, that is, we were not able to detect a pK_a for the deprotonation of a coordinated thiol, and thus we can exclude that NQI_2 represents a species where Cd^{II} is coordinated by a thiolate and a protonated thiol ligand. However, the decay from the monovalent Ag^{I} to the divalent Cd^{II} provides a considerable driving force for the deprotonation. Even at −196 °C it is possible that the proton would rapidly dissociate from the thiol group, possibly by tunnelling. Therefore, the results presented here cannot confirm nor reject the existence a coordinated thiol for the monovalent metal ions. Finally, we tested if chloride might coordinate in Ag^{I}-CueR, and this does not appear to be the case, see Figure S2. Similarly, we explored the effect of DNA binding and the presence of sucrose (used to limit the rotational diffusion), neither of which changed the NQI parameters significantly, and thus the observed structures were not affected, although the population of the two species may change, see Figures S3 and S4.

Scenario B: There is only one coordination geometry for Ag^{I} which relaxes into two different Cd^{II} coordination geometries via the radioactive decay. At −196 °C structural relaxation is limited for the atoms in the protein, but Cd^{II} may move, possibly with no barrier, to a local minimum on the free energy surface. Moreover, the β^- emission gives rise to a recoil energy of up to 557 kJ mol^{-1}, which may drive Cd^{II} into (two) different local energy minima, depending on the direction of the velocity vector with respect to the molecular structure. In Figure 5 we present a very simple analysis of the potential energy change upon moving Cd^{II} 0.5 Å from the position of Ag^{I} either along the S-Cd-S axis (*z*-axis) or within the equatorial plane. Clearly, the potential energy surface is relatively shallow for movement of Cd^{II} within the equatorial plane, while the potential energy rises steeply upon movement along the S-Cd-S axis. A recoil kinetic energy of some hundreds of kJ mol^{-1} may therefore give rise to considerable movement of Cd^{II}, if the velocity vector lies within equatorial plane, while a much larger energy barrier is encountered for movement along the S-Cd-S axis, as expected. Thus, in a very simple model, about 1/3 of the decays give rise to recoil along the *z*-axis, but the energy is quickly dissipated and Cd^{II} relaxes to the structure presented in Figure 4. The other 2/3 of the decays give rise to recoil in the equatorial plane, and the much lower potential energy change along this "reaction coordinate" allows Cd^{II} to be shifted to a different (local) energy minimum. This very simple model predicts a ratio of 1/2 of the two structures, in fair agreement with the observed ratio of amplitudes (2.3/7.4) of the two NQIs, see Table 1. In summary, we find scenario B more likely than scenario A.

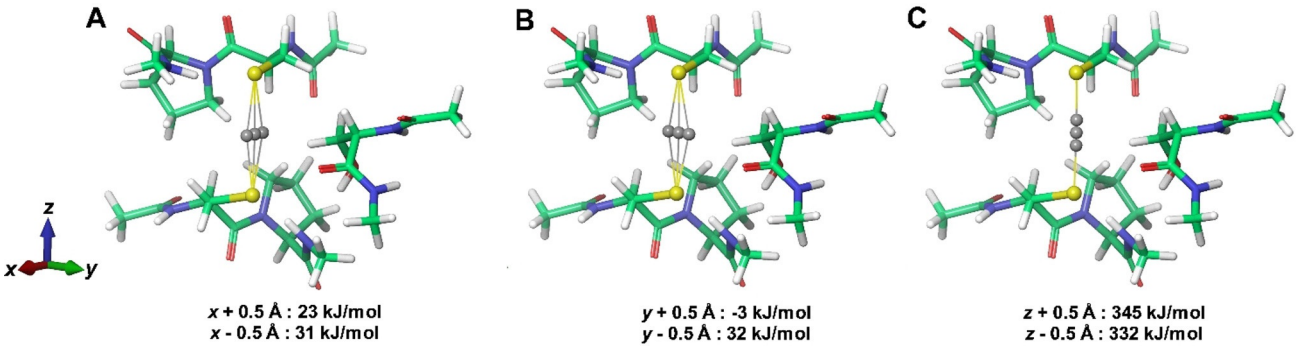

Figure 5. Change of potential energy upon translation of Cd^{II} away from the position occupied by Ag^{I} in CueR calculated using DFT (BP86/def2-T2VP). A) translation along *x*, B) translation along *y*, C) translation along *z* corresponding to S-Cd-S axis. Movement of Cd^{II} by 0.5 Å along the S-Cd-S axis gives rise to changes comparable to the recoil kinetic energy which ^{111}Cd receives in the nuclear decay, while the energy upon movement of 0.5 Å in the equatorial plane gives rise to potential energy changes which are an order of magnitude smaller.

The ^{111}Ag PAC experiment conducted at 1 °C exclusively displays one NQI, with essentially the same parameters as the low frequency NQI_2 observed at −196 °C. Consequently, this species must represent the lower free energy structure at 1 °C, and the barrier to relaxation from the high frequency species to the low frequency species must be small enough to be overcome within ≈10 ns at 1 °C. A simple estimate using transition state theory gives a barrier of less than 25 kJ mol^{-1}. The structural model with a water molecule relatively close to the metal site, and relaxation to a 3- or 4-coordinate structure, could account for the data recorded at 1 °C. To explore this further, we conducted a molecular dynamics (MD) simulation on CueR (PDB ID: 4WLW with Cu^{I} parameters), monitoring if a solvent molecule may be located in proximity of the metal ion at any time point. The shortest distance between water and Cu^{I} during 1 μS was 3.95 Å (Cu–O), see Figure 6. In this structure, there are multiple hydrogen bonds between the water molecule and hydrogen bond donors and acceptors within 4.0 Å of Cu^{I}, including the metal-coordinating C112 sulfur. Similarly, Rao et al. suggest that Zn^{II} bound to CueR may attract solvent water molecules to form a 4-coordinate site.[28] Thus, a solvent water molecule or other extraneous ligands may be present close to the metal ion, and potentially be recruited by Cd^{II} very quickly after the decay from ^{111}Ag to ^{111m}Cd, allowing for the formation of a 3- or 4-coordinate species.

From a theoretical chemistry point of view, the experimental data presented here may be modelled by placing Cd^{II} in the coordination geometry of Ag^{I}, and then simulating the dynamics of the system with an initial velocity (in addition to the Maxwell–Boltzmann kinetic energy) of Cd^{II} in a random direction and corresponding to a spectrum of recoil energies up to 557 kJ mol^{-1}. It is likely that this energy is rapidly dissipated (< 1 ps),[29,30] so the application of quantum mechanics based dynamics should be feasible, but it is beyond the scope of the current work.

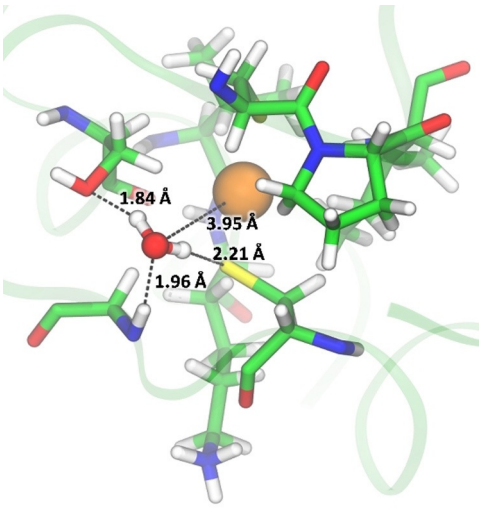

Figure 6. Structure selected from a 1 μs MD simulation on Cu^{I}-CueR (PDB ID: 4WLW) demonstrating that a solvent water molecule may approach the metal site, and, as an additional ligand, be attracted by Cd^{II} after the decay from ^{111}Ag.

^{111m}Cd decays to the nuclear ground state of ^{111}Cd, that is, it is an isomeric transition with no change of element or oxidation state, and ^{111m}Cd PAC spectroscopy therefore reflects the thermodynamic equilibrium of Cd^{II} binding to CueR. The ^{111m}Cd PAC spectrum of CueR exhibits low frequencies, see Figure 3 and Table 1, reflecting symmetric coordination, possibly distorted tetrahedral CdS_4, although other coordination geometries cannot be excluded. The C-terminal CCHH motif could provide the additional cysteines, in analogy to what has been proposed for Hg^{II} bound to CueR.[34] It is noteworthy that the ^{111}Ag and ^{111m}Cd PAC experiments at 1 °C give very different NQIs, demonstrating that the structure occupied by Cd^{II} at 1 °C derived from the ^{111}Ag spectrum is a transient species. The rotational correlation time of the protein, see Table 1, is the same in both experiments. The theoretical value for the global rotational correlation time is 1 μs^{-1}, using the Stokes–Einstein approximation for the rotational diffusion,[31] a molecular weight of the protein dimer of 30 500 Da, and a radius of hydration of 3 Å. This is slightly smaller than the experimental value of 6(4) μs^{-1}, implying that there may be a component of local dynamics contributing to the observed rotational diffusion, in agreement with the disordered metal ion binding loop observed by X-ray diffraction.[5] Thus dynamics affects the metal ion binding loop at the level of thermal energy. Moreover, the structure of the metal site changes upon a change of metal ion and oxidation state from Ag^{I} to Cd^{II}, where a considerably larger free energy change as well as recoil energy may be realized.

The flexibility of the CueR metal site reported in this work is likely to be an inherent facet of the protein function, where transcriptional activation is only desired for binding of the monovalent coinage metal ions, and other metal ions may disrupt the functional CueR binding site. This is in contrast to the metal site properties reported for the small blue copper protein azurin,[32] which is often described as exhibiting an entatic state.[21–23] Accordingly, only very little structural change was observed by ^{111}Ag PAC at the azurin metal site upon the decay from ^{111}Ag to ^{111}Cd.[32] It is remarkable that this correlates with the function of the two proteins: Azurin is an electron transporter, and is required to accommodate change of oxidation state between Cu^{I} and Cu^{II} without much structural reorganization, whereas CueR must essentially do the opposite, that is, discriminate against other metal ions binding to the same metal site. That is, not only the metal site structure, but also the metal site flexibility may be central to the function, and ^{111}Ag PAC spectroscopy may be applied to probe this property.

Conclusions

With this work we have probed the response of the Ag^{I}-CueR metal site to instantaneous change of element and oxidation state from Ag^{I} to Cd^{II}, due to the radioactive β-decay of ^{111}Ag to ^{111}Cd. Two coordination geometries are observed at low temperature (−196 °C). One which reflects Cd^{II} trapped in a distorted two-coordinate structure with an additional long contact to the S77 carbonyl oxygen, reminiscent of the site occupied by Ag^{I} bound to CueR. In the other structure Cd^{II} has at-

tracted one or more additional ligands, presumably because the recoil caused by the β^- emission is directed in the equatorial plane of the S-Cd-S structure. At 1 °C the structure rapidly relaxes this second species with higher coordination number. Nevertheless, the equilibrium Cd^{II} binding is different as probed by ^{111m}Cd PAC spectroscopy. This demonstrates that the CueR metal site is relatively flexible, and that Cd^{II} rapidly disrupts the functional S-Ag-S structure. In a more general perspective, ^{111}Ag PAC spectroscopy may be applied to probe the local potential energy surface near protein metal sites, because the Cd^{II} nucleus is equipped with recoil energy of a few hundred kJ mol^{-1} in the nuclear decay, that is, kinetic energy comparable to relevant chemical bond energies.

Experimental Section

Preparation of the ^{111}Ag solution

Metallic Pd powder (2.54 mg and 2.8 mg, respectively), enriched to 98.6% in ^{110}Pd (Oak Ridge National Lab, batch 214301) was enclosed in a quartz ampoule and irradiated for 4 days and 5 days, respectively in a thermal neutron flux of $(1.1–1.3)\times10^{15}$ cm^{-2}s^{-1} in the beam tube V4 of the high flux reactor at Institut Laue-Langevin in Grenoble, France. Thermal neutron capture on ^{110}Pd produces short-lived ^{111}Pd which beta-decays with 23.4 minutes half-life to ^{111}Ag. The samples were shipped to Hevesy Lab, Risø, Denmark, where radiochemical separation of ^{111}Ag from ^{110}Pd was carried out as described previously.[32]

Preparation of protein samples for PAC measurements

First, the radioactive ^{111}Ag or ^{111m}Cd solutions in 0.1 M HNO_3 were mixed with a non-radioactive $AgClO_4$ or $Cd(ClO_4)_2$ solution, respectively. The acidic metal ion solutions were neutralized with NaOH. Then, the CueR protein (in storage buffer 20 mM Tris/$HClO_4$, pH 7.5, 1 mM TCEP) and 35 bp P*copA* dsDNA (5′-AAAGGTTAAACCTTCCAGCAAGGGGAAGGTCAAGA-3′, in storage buffer 20 mM Tris/$HClO_4$, pH 8.0, 0.1 mM $NaClO_4$) were added. CueR was expressed in *E. coli* and purified as described previously.[33,34] Next, the pH was adjusted to the required value at RT by adding Tris or MES buffers and solutions of NaOH or $HClO_4$. Finally, sucrose (55% *w/w*) was dissolved into the mixtures in order to reduce the rotational diffusion of the protein.

To investigate the effect of the addition of Cl^- ions on the ^{111}Ag PAC spectra, NaCl ($c_{NaCl,stock}$ = 4 M) was added to a sample of Ag^I-CueR in a final concentration of 100 mM.

PAC measurements: Measurements were carried out at the University of Copenhagen with a PAC instrument consisting of six BaF_2 scintillation detectors.[35] During the measurements the temperature was maintained at 1 °C by a Peltier element or at −196 °C by liquid nitrogen.

PAC data evaluation: Evaluation of the PAC data was carried out using the Prelude32 and Winfit programs. 200 to 400 data points, depending on their information content, were used in the fitting procedures, except the first 7 points due to systematic errors experienced in these. Fourier transformation of the data and fits were carried out using a Keiser–Bessel window with a window parameter equal to 6. The time resolution and time per channel values were 0.981 ns and 0.562 ns, respectively. A component with pure exponential decay was included in the fit of the ^{111}Ag PAC data recorded at −196 °C with an amplitude of −0.009(1) and a decay rate of 22(9) μs^{-1}. This component is not included in Table 1, as it constitutes less than 10% of the total amplitude. The difference in amplitude of the ^{111}Ag experiments at −196 °C and 1 °C is a consequence of a shorter sample detector distance for the latter experiment. The ^{111}Ag spectrum at −196 °C presented in Figure 3 is a sum of several experiments, with and without sucrose and DNA, because they all gave the same two species (NQI_1 and NQI_2).

Ultrafiltration

In order to test if Ag^I was found in the protein fraction, a PAC Ag^I-CueR sample (without DNA) was treated as follows. First it was diluted with MilliQ water for reducing the viscosity (caused by the sucrose). The diluted sample was divided into two centrifugal filters (Vivaspin 500, 3 kDa MWCO, GE Healthcare) and centrifuged at 4 °C and 10 krpm for 160 min. The low M_w fractions from the two filters were pooled into one Eppendorf tube, and likewise for the high M_w fractions. The activity of the two fractions and the two inner cells of the ultrafilter units were measured with a PAC detector for 300 s. The sample—detector distance was 36.2 mm.

Molecular dynamics simulations

In order to examine solvent behaviour at the metal site, a 1 μs MD simulation of CueR (PDB ID: 4WLW) with Cu^I parameters was carried out using Desmond[36] and the OPLS3 force field.[37] The CueR complex was placed in a cubic box of TIP3P waters[38] ensuring a 15 Å solvent buffer on all sides of the complex. Na^+ counterions were automatically added to yield an overall charge neutral system. Desmond default settings were used for the NPT ensemble with thermostat and barostat set points of 300 K and 1 bar, respectively. Analysis of the MD trajectory and visualization was carried out with VMD.[39] The approach of water molecules to the Cu^I sites was analysed by parsing the MD trajectory in VMD, using a dynamically updated selection of all atoms within 4.5 Å of Cu^I during the simulation.

DFT calculations

DFT calculations on Cd^{II} model complexes (Figure 4 and 5) built from the PDB entry 4WLW were carried out with Orca 3.0.3.[40] During optimization the C120 and C112 side chains, S77 backbone, Cl^-, H_2O, metal ion, and hydrogen atoms were allowed to relax, while other atoms were frozen to their initial crystal structure positions. Optimizations were done using the BP86 functional[41] and the def2-TZVP basis set.[42,43] Electric field gradients (EFG) were calculated with the DKH2 relativistic approximation[44–46] using BHandHLYP[47] with def2-QZVPP on the metal ion and def2-TZVP on other atoms. Atom-pairwise dispersion corrections with the Becke–Johnson damping Scheme (D3BJ) were used in all DFT-calculations.[48,49]

Acknowledgements

Financial support from the Hungarian National Research, Development and Innovation Office (GINOP-2.3.2-15-2016-00038, and K 16/120130) is acknowledged.

Conflict of interest

The authors declare no conflict of interest.

Keywords: cadmium · flexibility · protein function · protein metal sites · relaxation · silver

[1] C. Rademacher, B. Masepohl, *Microbiology* **2012**, *158*, 2451 – 2464.
[2] K. Yamamoto, A. Ishihama, *Mol. Microbiol.* **2005**, *56*, 215 – 227.
[3] F. W. Outten, D. L. Huffman, J. A. Hale, T. V. O'Halloran, *J. Biol. Chem.* **2001**, *276*, 30670 – 30677.
[4] J. V. Stoyanov, J. L. Hobman, N. L. Brown, *Mol. Microbiol.* **2001**, *39*, 502 – 512.
[5] A. Changela, K. Chen, Y. Xue, J. Holschen, C. E. Outten, T. V. Halloran, A. Mondragón, *Science* **2003**, *301*, 1383.
[6] S. J. Philips, M. Canalizo-Hernandez, I. Yildirim, G. C. Schatz, A. Mondragón, T. V. O'Halloran, *Science* **2015**, *349*, 877 – 881.
[7] K. R. Brocklehurst, J. L. Hobman, B. Lawley, L. Blank, S. J. Marshall, N. L. Brown, A. P. Morby, *Mol. Microbiol.* **1999**, *31*, 893 – 902.
[8] Z. Ma, F. E. Jacobsen, D. P. Giedroc, *Chem. Rev.* **2009**, *109*, 4644 – 4681.
[9] N. L. Brown, J. V. Stoyanov, S. P. Kidd, J. L. Hobman, *FEMS Microbiol. Rev.* **2003**, *27*, 145 – 163.
[10] C. C. Chang, L. Y. Lin, X. W. Zou, C. C. Huang, N. L. Chan, *Nucleic Acids Res.* **2015**, *43*, 7612 – 7623.
[11] D. Wang, S. Huang, P. Liu, X. Liu, Y. He, W. Chen, Q. Hu, T. Wei, J. Gan, J. Ma, H. Chen, *Sci. Rep.* **2016**, *6*, 33391.
[12] X. Liu, Q. Hu, J. Yang, S. Huang, T. Wei, W. Chen, Y. He, D. Wang, Z. Liu, K. Wang, J. Gan, H. Chen, *Proc. Natl. Acad. Sci. USA* **2019**, *116*, 20398.
[13] M. M. Ibáñez, S. K. Checa, F. C. Soncini, *J. Bacteriol.* **2015**, *197*, 1606.
[14] J. V. Stoyanov, N. L. Brown, *J. Biol. Chem.* **2003**, *278*, 1407 – 1410.
[15] D. Szunyogh, H. Szokolai, P. W. Thulstrup, F. H. Larsen, B. Gyurcsik, N. J. Christensen, M. Stachura, L. Hemmingsen, A. Jancsó, *Angew. Chem. Int. Ed.* **2015**, *54*, 15756 – 15761; *Angew. Chem.* **2015**, *127*, 15982 – 15987.
[16] L. Hemmingsen, K. N. Sas, E. Danielsen, *Chem. Rev.* **2004**, *104*, 4027 – 4062.
[17] A. Jancso, J. G. Correia, A. Gottberg, J. Schell, M. Stachura, D. Szunyogh, S. Pallada, D. C. Lupascu, M. Kowalska, L. Hemmingsen, *J. Phys. G* **2017**, *44*, 064003.
[18] R. B. King, *Encyclopaedia of Inorganic Chemistry, Vol. 2*, Wiley, England, **1994**.
[19] M. Hargittai, *Chem. Rev.* **2000**, *100*, 2233 – 2302.
[20] F. Hanke, S. Hindley, A. C. Jones, A. Steiner, *Chem. Commun.* **2016**, *52*, 10144 – 10146.
[21] W. R. Hagen, *Metallomics* **2019**, *11*, 1768 – 1778.
[22] B. Dicke, A. Hoffmann, J. Stanek, M. S. Rampp, B. Grimm-Lebsanft, F. Biebl, D. Rukser, B. Maerz, D. Göries, M. Naumova, M. Biednov, G. Neuber, A. Wetzel, S. M. Hofmann, P. Roedig, A. Meents, J. Bielecki, J. Andreasson, K. R. Beyerlein, H. N. Chapman, C. Bressler, W. Zinth, M. Rübhausen, S. Herres-Pawlis, *Nat. Chem.* **2018**, *10*, 355 – 362.
[23] J. Stanek, A. Hoffmann, S. Herres-Pawlis, *Coord. Chem. Rev.* **2018**, *365*, 103 – 121.
[24] R. Bauer, S. J. Jensen, B. Schmidt-Nielsen, *Hyperfine Interact.* **1988**, *39*, 203 – 234.
[25] H. Haas, S. P. A. Sauer, L. Hemmingsen, V. Kellö, P. W. Zhao, *Europhys. Lett.* **2017**, *117*, 62001.
[26] K. Chen, S. Yuldasheva, J. E. Penner-Hahn, T. V. O'Halloran, *J. Am. Chem. Soc.* **2003**, *125*, 12088 – 12089.
[27] R. Zhang, J.-S. McEwen, *J. Phys. Chem. Lett.* **2018**, *9*, 3035 – 3042.
[28] L. Rao, Q. Cui, X. Xu, *J. Am. Chem. Soc.* **2010**, *132*, 18092 – 18102.
[29] J. Jolie, N. Stritt, H. G. Börner, C. Doll, M. Jentschel, S. J. Robinson, E. G. Kessler, *Z. Phys. B* **1996**, *102*, 1 – 7.
[30] N. Stritt, J. Jolie, M. Jentschel, H. G. Börner, C. Doll, *Phys. Rev. B* **1998**, *58*, 2603 – 2613.
[31] R. Fromsejer, L. Hemmingsen, *Hyperfine Interact.* **2019**, *240*, 88.
[32] R. Bauer, E. Danielsen, L. Hemmingsen, M. J. Bjerrum, Ö. Hansson, K. Singh, *J. Am. Chem. Soc.* **1997**, *119*, 157 – 162.
[33] R. K. Balogh, B. Gyurcsik, É. Hunyadi-Gulyás, H. E. M. Christensen, A. Jancsó, *Protein Expression Purif.* **2016**, *123*, 90 – 96.
[34] R. K. Balogh, B. Gyurcsik, É. Hunyadi-Gulyás, J. Schell, P. W. Thulstrup, L. Hemmingsen, A. Jancsó, *Chem. Eur. J.* **2019**, *25*, 15030 – 15035.
[35] T. Butz, S. Saibene, T. Fraenzke, M. Weber, *Nucl. Instrum. Methods Phys. Res., Sect. A* **1989**, *284*, 417 – 421.
[36] K. J. Bowers, E. Chow, H. Xu, R. O. Dror, M. P. Eastwood, B. A. Gregersen, J. L. Klepeis, I. Kolossvary, M. A. Moraes, F. D. Sacerdoti, J. K. Salmon, Y. Shan, D. E. Shaw, *Scalable Algorithms for Molecular Dynamics Simulations on Commodity Clusters*, Association for Computing Machinery, Tampa, Florida **2006**.
[37] E. Harder, W. Damm, J. Maple, C. Wu, M. Reboul, J. Y. Xiang, L. Wang, D. Lupyan, M. K. Dahlgren, J. L. Knight, J. W. Kaus, D. S. Cerutti, G. Krilov, W. L. Jorgensen, R. Abel, R. A. Friesner, *J. Chem. Theory Comput.* **2016**, *12*, 281 – 296.
[38] W. L. Jorgensen, J. Chandrasekhar, J. D. Madura, R. W. Impey, M. L. Klein, *J. Chem. Phys.* **1983**, *79*, 926 – 935.
[39] W. Humphrey, A. Dalke, K. Schulten, *J. Mol. Graphics* **1996**, *14*, 33 – 38.
[40] F. Neese, *WIREs Comput. Mol. Sci.* **2012**, *2*, 73 – 78.
[41] A. D. Becke, *Phys. Rev. A* **1988**, *38*, 3098 – 3100.
[42] A. Schäfer, H. Horn, R. Ahlrichs, *J. Chem. Phys.* **1992**, *97*, 2571 – 2577.
[43] F. Weigend, R. Ahlrichs, *Phys. Chem. Chem. Phys.* **2005**, *7*, 3297 – 3305.
[44] R. J. Buenker, P. Chandra, B. A. Hess, *Chem. Phys.* **1984**, *84*, 1 – 9.
[45] B. A. Hess, *Phys. Rev. A* **1985**, *32*, 756 – 763.
[46] B. A. Hess, *Phys. Rev. A* **1986**, *33*, 3742 – 3748.
[47] A. D. Becke, *J. Chem. Phys.* **1993**, *98*, 1372 – 1377.
[48] S. Grimme, S. Ehrlich, L. Goerigk, *J. Comput. Chem.* **2011**, *32*, 1456 – 1465.
[49] S. Grimme, J. Antony, S. Ehrlich, H. Krieg, *J. Chem. Phys.* **2010**, *132*, 154104.

Manuscript received: January 10, 2020
Accepted manuscript online: February 11, 2020
Version of record online: May 19, 2020

